

Title: The rhodopsin-guanylyl cyclase of the aquatic fungus *Blastocladiella emersonii* enables fast optical control of cGMP signaling

Authors: U. Scheib^{1†}, K. Stehfest^{1†}, C. E. Gee^{2†}, H. G. Körschen³, R. Fudim¹, T. G. Oertner^{2*}, and P. Hegemann^{1*}

One Sentence Summary: We describe a light-activated guanylyl cyclase that can be used for optogenetic control of cGMP.

Affiliations:

¹Institute for Biology, Experimental Biophysics, Humboldt-Universität zu Berlin, D-10115 Berlin, Germany.

²Institute for Synaptic Physiology, Center for Molecular Neurobiology Hamburg, University Medical Center Hamburg-Eppendorf, D-20251 Hamburg, Germany.

³Center of Advanced European Studies and Research (caesar), Department Molecular Sensory Systems, Ludwig-Erhard-Allee 2, 53175 Bonn, Germany.

[†]equal contribution

*Corresponding authors: hegemann@rz.hu-berlin.de (P.H.) and thomas.oertner@zmn.uni-hamburg.de (T.G.O.)

Abstract:

Blastocladiomycota fungi form motile zoospores that are guided by sensory photoreceptors to optimal light conditions. Here we show that the microbial rhodopsin of *Blastocladiella emersonii* is a rhodopsin-guanylyl cyclase (RhGC). RhGC is the first member of a new rhodopsin class of light-activated enzymes. Upon light absorption, RhGC (D525) converts in 8 ms after a light flash into a blue-shifted signaling state P380 and recovers within 100 ms. RhGC was well expressed and produced cGMP in response to green light in *Xenopus* oocytes, CHO cells, and mammalian neurons. Cyclic GMP production was light dose-dependent, rapid and reproducible. Thus, RhGC is a versatile tool for optogenetic analysis of cGMP-dependent signaling processes in cell biology and the neurosciences.

[Main Text:]

Introduction

Nature has developed very few classes of principle sensory photoreceptors, namely the rhodopsins, flavoproteins and phytochromes that are used by living organisms to orient in an illuminated world. Rhodopsins are used for photosensing whenever speed is required. Until now three classes of rhodopsins have been identified: the sensory rhodopsins that activate G-proteins or His-kinases, the light-activated ion channels (channelrhodopsins), and the light-driven ion pumps (1). Spores of fungi in the family *Blastocladiaceae* are phototactic requiring cGMP and retinal for photoorientation, and showing action spectra for photoorientation that are rhodopsin-like (2-4). In the genome of *Blastocladiella emersonii*, a microbial rhodopsin sequence has been recently identified (4). The authors showed that this protein is expressed in the eyespot of the *Blastocladiella* zoospore and phototactic experiments provided compelling evidence that this rhodopsin is functioning as the phototaxis photoreceptor (4). Furthermore, sequence analysis revealed that the *Blastocladiella* rhodopsin is directly connected to a putative guanylyl cyclase (GC) domain through a 46 amino acid linker (Fig. 1A). An interspersed kinase homologous module, which connects most other membrane bound GCs to their transmembrane helix (5) is absent.

Since such rhodopsin-enzyme hybrids have never been found before, we characterized the newly discovered rhodopsin-guanylyl cyclase (RhGC) spectroscopically and electrophysiologically in heterologous expression systems. Finally, we coexpressed RhGC together with the cGMP activated CNG-A2 channel in CHO cells and hippocampal neurons and confirmed the suitability of RhGC as a novel optogenetic tool to control intracellular cGMP levels.

Results

Characterization of RhGC in *Xenopus* oocytes

We expected that heterologous expression of the RhGC protein would be sufficient to enable optical control of cGMP levels in cells. To test this hypothesis, we expressed codon-humanized RhGC-encoding RNA together with RNA for a cGMP-gated channel CNG-A2 from rat olfactory neurons ($K_{1/2}^{cAMP}=36\ \mu\text{M}$, $K_{1/2}^{cGMP}=1.3\ \mu\text{M}$) (6) in *Xenopus laevis* oocytes. Three to five days after RNA injection, we analyzed photocurrents in oocytes supplemented with *all-trans* retinal. Based on the phototaxis action spectrum (4), cells were illuminated for 2 seconds with 560 nm light. Inward currents gradually increased with light intensity (Fig. 1B) and current slopes saturated with a half maximal light intensity $EC_{50}=0.028\ \text{mW mm}^{-2}$ (Fig. 1C). Varying the light pulse duration (0.1 - 1.6 s of 530 nm light) produced photocurrents of graded amplitude but nearly constant slope (Fig. 1, D and E). The onset was $390 \pm 35\ \text{ms}$ after light-on and the delay between light-off and peak photocurrent was $1.9 \pm 0.072\ \text{s}$ ($n=6$). After switching on the light, the currents continued to increase with no signs of saturation for as long as 30 s at the light intensities used (Fig. 1F). We tested the specificity of the cyclase by coexpressing RhGC with the CNG-A2 channel mutant C460W/E583M, which is more sensitive to cAMP compared with cGMP ($K_{1/2}^{cAMP}: 0.89\ \mu\text{M}$, $K_{1/2}^{cGMP}: 6.2\ \mu\text{M}$) (6). Photocurrents were less than 1% compared with the cGMP-gated CNG-A2 channel experiments demonstrating that RhGC is highly selective for GTP (Fig. 1G). In addition, the lack of photocurrents in the absence of the cGMP sensitive channel illustrates that RhGC does not possess substantial ion channel or ion pumping activity. In control experiments with oocytes coexpressing the cAMP-channel with the photo-activated adenylyl cyclase bPAC (7) blue light of 450 nm evoked long lasting photocurrents, confirming the functionality of the cAMP-channel.

Next, we determined the cGMP concentrations in oocytes by employing a competitive immunoassay (Fig. 1H). Five days after RNA injection, 0.2 ± 0.04 pmol cGMP were extracted from dark-adapted cells (mean of $n = 11$ experiments), a value only slightly above control cells (0.1 ± 0.01 pmol/oocyte, $n = 6$ experiments). However, after 5 min green illumination (530 nm, 0.01 mW mm^{-2}), cGMP increased ca. 100-fold to 22.1 ± 1.6 pmol/oocyte ($n = 12$ experiments). The actual dynamic range of RhGC might be even larger since the cGMP concentration in the cell depends on the activity of both cyclases and esterases. Expression of a RhGC with truncated N-terminus (-138 aa, see fig. S1) showed ~ 20 fold reduced photocurrent amplitudes (Fig. 1B, red trace) and ~ 6 fold reduced cGMP levels, suggesting that the N-terminus plays a role for cyclase function, cyclase activation, and/or RhGC folding and trafficking to the membrane. The concentration of cAMP was not affected by illumination (Fig. 1I), corroborating the high GTP selectivity of RhGC found in the electrical measurements (Fig. 1, B to G). Conversely, cAMP levels increased in bPAC expressing cells upon blue illumination (470 nm, 0.015 mW mm^{-2}).

Activation of RhGC in CHO cells

To analyze RhGC activity in mammalian cells, we created a CHO K1 cell line stably expressing mCherry-tagged RhGC with a cGMP sensitive CNG-A2 channel ($K_{1/2}^{\text{cAMP}} = 14 \text{ }\mu\text{M}$, $K_{1/2}^{\text{cGMP}} = 0.7 \text{ }\mu\text{M}$) (8). Calcium levels, reported by Fluo-4 or Fura-2 fluorescence increased strongly upon repetitive 485 nm flashing with the Xenon lamp of the plate reader in a dose-dependent manner (Fig. 2A). The light-induced $[\text{cGMP}]_i$ increase was fully reversible without major adaptation (Fig. 2B).

Characterization of recombinant RhGC

Sequence alignment of the RhGC rhodopsin fragment (Rh) of *B. emersonii* with other rhodopsins (fig. S1) and a 3D model based on the structure of sensory rhodopsin NpSRII (fig. S2) revealed that *B. emersonii* Rh is a typical microbial rhodopsin with a retinal-binding pocket for all-trans retinal and a conserved active site (fig. S1 and S2).

To assess the spectral properties of RhGC, we purified the recombinant rhodopsin-fragment (Rh) (aa 1-396, fig. S1) from the methylotrophic yeast *Pichia pastoris*. The full-length RhGC could not be purified in sufficient amounts. Dark-adapted Rh shows a typical unstructured rhodopsin spectrum with a maximum at 525 nm (D525, Fig. 3A). Bright green illumination (530 nm) converted D525 into a species with deprotonated chromophore absorbing maximally at 380 nm (P380), which we considered as the main photocycle intermediate and most likely the signaling state. After short illumination (5 s), P380 fully converted back to D525 whereas after long illumination (5 min) a substantial Rh fraction did not recover, probably due to reduced stability of the photoproducts in detergent (Fig. 3A). Stimulation with a 10 ns laser flash unveiled the reversible dynamics of the photocycle. P380 is formed with $\tau = 8$ ms after flash and reverts with $\tau = 93$ ms at 22 °C and pH = 8 (Fig. 3B). However, depletion and recovery kinetics of the dark state monitored at 505 and 550 nm were both biexponential suggesting the existence of additional photoproducts prior to and after P380 (Fig. 3 and Table 1). To address this question we recorded a series of spectra between 350 nm and 650 nm after laser stimulation (Fig. 3C). Beyond P380 the spectra revealed an early red-shifted photoproduct, P580, that converted into P380 within 8 ms. *Pichia* membranes with full-length RhGC were used for further characterization of the cyclase activity. We found that in the light, RhGC exhibited a very stable

activity with an initial velocity of 1 nmol cGMP per second and nmol RhGC at 1 mM GTP RhGC, whereas in darkness RhGC is totally inactive (at least 10.000 fold less active compared to light) (Fig. 3D, see M.M. for calculation).

RhGC expression in hippocampal neurons

As proof of concept for optogenetic applications, we tested RhGC function in hippocampal CA1 neurons (Fig. 4A). Bright green light activated endogenous currents of less than -20 pA in neurons expressing RhGC (Fig. 4B, -11.7 ± 2.8 pA, $n = 3$). When the cGMP activated channel CNG-A2 was co-expressed with RhGC, large inward currents were evoked by green light (Fig. 4B). Therefore, light-activated RhGC increased neuronal cGMP levels and activated CNG-A2 in CA1 neurons. The almost complete absence of currents in neurons expressing RhGC alone, demonstrates that CA1 neurons have almost no endogenous cGMP activated channels and that RhGC does not itself have substantial ion channel or ion pumping activity. The activation spectrum showed a peak at around 530 nm (Fig. 4, C and D) consistent with the absorption spectrum of dark-adapted RhGC (Fig. 3A). Light pulses applied every 5 s yielded photocurrents of very reproducible amplitude (Fig. 4E). Dendritic morphology of CA1 neurons expressing RhGC, CNG-A2 and the far-red fluorescent protein mKate2 was indistinguishable from CA1 cells expressing mKate2 only (Fig. 5A). Transfected neurons showed normal resting membrane potential and spiking behavior in response to depolarizing current steps (Fig. 5, B and C). RhGC expression is therefore well tolerated in neurons suggesting good folding and low or no dark activity. Photocurrent amplitude depended on light intensity (Fig. 5D). The light sensitivity of RhGC-expressing cells (Fig. 5E) was comparable to the sensitivity of ChR2 expressing cells ($EC_{50} \approx 1.1$ mW mm⁻²) (9). Varying the duration of saturating light pulses (19.2 mW mm⁻²)

resulted in photocurrents with uniform slope but graded amplitude (Fig. 5F). The time to onset of the currents was 120 ± 30 ms, ($n = 7$, median 85 ms, see Fig. 5F). Therefore, [cGMP]_i can be optogenetically controlled in a quantitative, reversible and reproducible fashion in mammalian neurons.

Discussion

With the experiments described above we validate the hypothesis that the microbial rhodopsin of the fungus *Blastocladiella emersonii* is functioning as a directly light-activated guanylyl cyclase. To sense light, this fungus has developed a unique light sensor that combines the function of a light-absorbing rhodopsin and highly specific cyclase into a single molecule, without the need for a transducer intermediary. This strategy is different from all other behavioral photoreceptor transduction cascades described so far.

By successful expression and functional characterization in three different heterologous systems we show that RhGC has the potential to become a widely used optogenetic tool for the exploration of cGMP signaling. Cyclic GMP is an important signaling molecule in many eukaryotes including mammals. Vision and olfaction depend critically on cGMP, as well as muscle contraction, homeostasis and cardiovascular function (11). Optical control of the cGMP system would be very desirable, although a photoactivated guanylyl cyclase (BlgC) engineered from bPAC has been described (12). BlgC, however, possesses a significant dark activity and still possesses ~10% residual adenylyl cyclase activity *in vitro*. In contrast, we detected no adenylyl cyclase activity of RhGC in oocytes, indicating a high selectivity for GMP. Furthermore, our *in vitro* assay with recombinant RhGC shows that the enzyme is totally inactive in darkness. Another advantage of rhodopsins over flavin-based photoreceptor domains is the

possibility of tuning the absorption wavelength and kinetic properties to suit the experimental demands (14, 15). Similar to channelrhodopsins, RhGC can be activated repetitively without obvious bleaching effects, an important feature for reproducible optical stimulation.

Materials and Methods

Molecular biology

A full-length human codon-optimized DNA sequence encoding RhGC of *Blastocladia emersonii* (accession no. KP731361, a humanized version of KF309499) was purchased from Genscript, cloned via BamHI and Hind3 into pGEM (Promega), and used for cRNA synthesis. For expression of RhGC in CHO K1 cells, the 3' end of the RhGC cDNA was fused to the mCherry and cloned via XbaI and BamHI into the pcDNA6/V5-HIS A vector (Life technologies). The resulting construct was designated pc6RhGC-mCherry.

Characterization of RhGC in *Xenopus* oocytes

Oocytes were prepared from female *Xenopus laevis* as described previously (15). Single oocytes were injected with different cRNA combinations and incubated in Ringer solution supplemented with 1 μ M all-trans-retinal (Sigma, St. Louis, MO). RhGC was coexpressed with the cGMP sensitive CNG-A2 channel (rat olfactory, gb: 6978671 6 or the cAMP sensitive version (C460W/E583M). Therefore, 2.5 ng RhGC or trRhGC cRNA were coinjected with 5 ng cGMP sensitive CNG cRNA (Fig. 1, B and C); 5 ng of each cRNA was used for Fig. 1, D to F. For Fig. 1G, 5 ng RhGC cRNA, together with 5 ng of the cAMP sensitive CNG channel was injected. Control cells were injected with 100 pg bPAC and 20 ng of the cAMP sensitive CNG variant

(Fig. 1G). Photocurrents were measured 3–5 days after RNA injection. For two-electrode voltage-clamp measurements and data acquisition we used a Turbo Tec-03X amplifier (NPI Electronic, Tamm, Germany) and pClamp 9.0 (Molecular Devices, Eugene, OR). Microelectrodes were fabricated from borosilicate glass capillaries (1.50 mm O.D. and 1.17 mm I.D.) using a micropipette puller (model No. P-97; Sutter instruments, Novato, CA) and filled with 3 M KCl. Microelectrode resistance was 0.5–1.5 M Ω . Actinic light of a XBO 75W Xenon lamp (Osram, Munich, Germany) was controlled by an LS3 shutter (Vincent Associates UNIBLITZ, Rochester, NY) and filtered by a 560 nm wideband filter (K55 Balzers, half bandwidth: 60 nm) or a 530 nm filter (20BPF10-530 8C057 Newport, half bandwidth: 9 nm). Light intensity was decreased with the help of neutral density filters. The composition of the extracellular buffer was (in mM): 96 NaCl, 5 KCl, 0.1 CaCl₂, 1 MgCl₂, 5 HEPES, pH 7.5. Oocytes were voltage clamped at -20 mV or -40 mV. The functionality of the cAMP sensitive CNG channel (C460W/E583M) was shown through coexpression with bPAC and 3 s illumination with 450 nm light of 0.03 mW mm⁻². Data were analyzed with Stimfit 0.13 (16) and Clampfit 10.4 (Molecular Devices LLC).

ELISA Assays

Five days after cRNA injection (10 ng RhGC or tr RhGC, 100 pg (Fig 1H) or 1 ng bPAC (Fig 1I), control cells: non-injected) three of the respective oocytes were pooled and either kept in dark or illuminated with 522 nm (0.010 mW mm⁻²) or 470 nm (0.015 mW mm⁻²) light of a LED Array (Adafruit NeoPixel NeoMatrix 8x8 - 64 RGB). Oocytes were disrupted in 300 μ l 0.1 M HCl by vigorous pipetting. Cell debris and protein (>10 kd) was removed through 3 successive centrifugation steps at 4 °C: 1) 7 min at 16.000 rpm, 2) 7 min at 15.000 rpm using a 0.22 μ m

Spin-X cellulose acetate membrane centrifugal filter (Corning Costar), and 3) 30 min at 14.000 rpm using a Ultra-0.5 Centrifugal Filter with Ultracel-10 membrane (Amicon). The amount of cGMP in the purified lysate was determined through a direct cGMP ELISA assay following the manufacturer's instructions (Enzo life sciences). To calculate cGMP levels an oocyte volume of 1 μ l was assumed. Mean values and standard errors of individual samples (n between 2 and 10) derived from three different frogs are shown in Fig. 1H. For the cAMP analysis of Fig. 1I, illumination and lysate purification was performed as described above with the help of a direct cAMP ELISA assay (Enzo life sciences).

Generation of Stable Cell Lines

CHO K1 cells stably expressing a CNG-A2 channel-based cGMP sensor (8) were electroporated with pc6RhCG-mCherry using the Neon 100 kit (Invitrogen) and a MicroPorator (Digital Bio) according to the manufacturer's protocol (3 x 1,650 mV pulses with 10 ms pulse width). Cells were transferred into complete medium composed of F12 plus GlutaMax (Invitrogen) and 10% fetal bovine serum (Biochrom). For the selection of monoclonal cells stably expressing RhGC, the antibiotics G418 (400 μ g/ml; Invitrogen) and Blasticidin (50 μ g/ μ l; Invitrogen) were added 24 h after electroporation. Monoclonal cell lines were identified by fluorescence microscopy using mCherry expression.

Fluorescence-based RhGC assays

The activity of heterologously expressed RhGC in CHO K1 cells was monitored using a cGMP sensitive CNG-A2 channel and Fluo-4 or Fura-2 (Life technologies). Assays were performed in

96-well plates (Greiner) using a Fluostar Omega reader (BMG Labtech) at 29 °C. Ratiometric Fura-2 measurements were performed using 340 nm/ 380 nm excitation and 510 nm emission. For Fluo-4 measurements, 485 nm and 520 nm filters were used for excitation and emission, respectively. All bandpass filters had a half bandwidth of 10 nm. RhGC was stimulated by the 485 nm flashes of the plate reader's Xenon-lamp or by an external light source (0.0013 mW mm⁻², 530 nm). Stimuli of different strength were achieved by varying the number of flashes. Data analysis was performed using the reader software MARS (BMG Labtech) and Origin software (Origin Lab Corp.).

Spectroscopy on recombinant protein

For heterologous expression of full-length RhGC and Rh domain (1-396 aa) in *Pichia pastoris* cells (strain 1168H, Invitrogen), DNA sequences were cloned in the pPICZ vector (Invitrogen) via EcoRI and NotI restriction sites that contains a C-terminal polyhistidine tag (6HIS). Transformation, cell culture and protein purification were performed as described before (17). After induction of protein expression for 24 h, cells were harvested and gently lysed using a high pressure homogenizer (Avestin). The membrane fraction of Rh was collected, homogenized and solubilized in 1 % (w/v) dodecylmaltoside (DDM). After binding of Rh protein to Ni-NTA resin (5 mL-HIS trap crude column, GE Healthcare) and washing of the column with 10 column volumes of 50 mM imidazole, Rh was eluted with 500 mM imidazole. Fractions that contained the protein were pooled, desalted (Hiprep 26/10 desalting column, GE Healthcare) and concentrated (Amicon Ultra 100 kDa, Millipore) in Tris-buffer (50 mM Tris, pH 8.0, 100 mM NaCl, 0.03 % DDM, 0.1 mM PMSF) to an optical density of 1 at 525 nm. Spectra were recorded in a Cary 50 Bio spectrophotometer (Varian, Inc., Darmstadt, Germany) at 20 °C at a spectral

resolution of 1.6 nm. Light spectra were recorded after 1 min illumination with a green LED (505 nm, 0.07 mW mm⁻²).

Transient spectroscopy was performed on an LKS.60 flash photolysis system (Applied Photophysics Ltd., Leatherhead, UK) at 22 °C. Excitation pulses of 10 ns (525 nm) were provided by a tunable Rainbow OPO/Nd:YAG laser system. Laser energy was adjusted to 6 mJ/shot. The instrument used a Xe-Lamp (150 W) as monitoring light source, which was pulsed during short time experiments. Data analysis was performed with Matlab 7.01 (The MathWorks, Natick, MA). Singular value decomposition of representative data sets was performed to identify significant components that were used for reconstruction of the three-dimensional spectra. Time constants were obtained by fitting exponential functions to the data.

HPLC Assay of cGMP

The membrane of RhGC expressing *Pichia pastoris* was prepared as described above with Tris-buffer containing 5 mM MnCl₂ and 0.1 mM GTP to stabilize the protein. After centrifugation, membranes were washed in Tris-buffer without GTP. Catalytic activity was measured at 25 °C in 100 µL Ringer solution with 1.5-1 mg total membrane protein. Samples were kept in the dark or were illuminated with 522 nm light of 0.01 mW mm⁻² (LED array, Adafruit NeoPixel NeoMatrix 8x8 - 64 RGB). Reactions were started by adding 1 mM GTP. Aliquots were taken at different time points and were immediately frozen in liquid nitrogen. 200 µL of 0.1 N HCl was added and thawed samples were centrifuged and filtered (0.2 µm pore-size, Chromafil; Machery-Nagel) to remove the membrane and denatured protein. Nucleotides were separated by HPLC using a C18 reverse-phase column (Supelco, Sigma-Aldrich) and 100 mM potassium phosphate, pH 5.9, 4 mM tetrabutylammoniumiodide, 10% (v/v) methanol as eluent. Nucleotides were monitored at

253 nm. Data were analyzed with Origin software (Origin Lab Corp.). Peak areas of GTP and cGMP were assigned and integrated by comparing retention times with the corresponding standard compounds. Due to slight fluctuation of the cGMP dark values, we determined the degree of cyclase light activation by comparing the cGMP produced in the light after 120 seconds with the dark value after 64800 seconds (Fig. 3C). The amount of cGMP increased with light exposure ($p < 0.02$, Spearman correlation = 1) but did not change in the dark ($p = 0.7$, Spearman correlation = 0.26). The amount of RhGC (M=69000 Da) was determined by calculating the amount from Coomassie-stained SDS-Page gel in comparison to a known amount of a reference protein. A direct absorption measurement of purified full-length RhGC was not possible since in our hands the functional full-length protein could not be solubilized from the membrane yet.

Electrophysiology of hippocampal neurons

Hippocampal slice cultures from female Wistar rats were prepared at postnatal day 5–6 as described (18). No antibiotics were used in the preparation or culture medium. The following plasmids were prepared with the neuron-specific promoter Synapsin-1 (syn): pAAV-syn-beRHGC-2A-timer2 (RhGC), rat CNG-A2 (PCI-syn-CNGA2), PCI-syn-mKate2N. RhGC and CNG-A2 plasmids were diluted to 25 ng/ μ l and mKate2 to 50 ng/ μ l in K-gluconate based pipette solution consisting of (in mM): 135 K-gluconate, 4 MgCl₂, 4 Na₂-ATP, 0.4 Na-GTP, 10 Na₂-phosphocreatine, 3 ascorbate, and 10 HEPES (pH 7.2, 295 mOsm, electroporation pipette resistance \sim 14 M Ω). Slices were submerged in solution containing (in mM): 145 NaCl, 10 HEPES, 25 D-Glucose, 2.5 KCl, 1 MgCl₂, 2 CaCl₂ (pH 7.4, \sim 311 mOsm). An Axoporation 800A (Molecular Devices, Sunnyvale CA) was used to deliver the DNA to loosely patched neurons (50

pulses (-12 mV, 0.5 ms) at 50 Hz) (19). After 4-10 days of expression, whole-cell patch-clamp recordings were established at 30 °C in artificial cerebrospinal fluid (ACSF) containing (in mM): 127 NaCl, 2.5 KCl, 2 CaCl₂, 1 MgCl₂, 25 NaHCO₃, 1.25 NaH₂PO₄, 25 D-glucose (pH 7.4, ~308 mOsm, saturated with 95% O₂ / 5% CO₂). In most experiments NBQX (10 μM), CPPene (10 μM) and picrotoxin (100 μM) were added to block fast excitatory and inhibitory synaptic transmission. Recording pipettes (3 - 6 MΩ) were filled with the same intracellular solution used for electroporation (without the DNA). Cells were voltage clamped at -65 mV and currents recorded with an Axoclamp200B (Molecular Devices) and Ephys software (20). Series resistance was less than 20 MΩ. For photostimulation of RhGC, a 4-LED light source (Mightex, Toronto, Canada) was coupled to the camera port of a BX61WI Microscope (Olympus, Tokyo Japan) via a multimode fiber (1.0 mm) and collimator (Thorlabs, Newton NJ). Radiant power was measured with a Si photodiode (LaserCheck, Coherent Santa Clara CA) in the specimen plane (objective used, Plan-Apochromat 40x 1.0NA, Zeiss, Jena Germany) and divided by the illuminated field (0.244 mm²). For determining the action spectra, the illumination intensity from the 4 color LEDs were set to match as closely as possible and the currents divided by the actual intensity to correct for small variations between LEDs prior to normalization. Analysis of the currents was performed using Matlab, graphs and curve-fitting were generated using GraphPad Prism 6.0.

Data analysis and statistics

All data are reported as means ± SEM derived from at least three independent biological experiments, unless otherwise stated in the figure legends or results sections. Statistical analyses and curve-fitting were performed using GraphPad Prism 6.0 or OriginPro 8G. Non-parametric tests were preferentially used. For comparing cGMP and cAMP amounts (Fig. 1, H and I) a

Kruskal-Wallis test was performed followed by Mann-Whitney pair-wise comparisons. For the comparison of cGMP formation in dark-adapted and illuminated RhGC containing membranes, unpaired t-tests with a Holm-Sidak correction for multiple comparisons was applied following determination of the Spearman correlation coefficient (Fig 3D). *P* values < 0.05 were considered significant.

Supplementary Materials

Fig. S1. Alignment of the RhGC rhodopsin domain.

Fig. S2. 3D model of the RhGC rhodopsin active site based on the NpSRII structure.

References and Notes

1. O. P. Ernst, D. T. Lodowski, M. Elstner, P. Hegemann, L. S. Brown, H. Kandori, Microbial and animal rhodopsins: structures, functions, and molecular mechanisms. *Chem Rev* **114**, 126-163 (2014).
2. P. M. Silverman, Regulation of Guanylate Cyclase Activity during Cytodifferentiation of *Blastocladiella Emersonii*. *Biochemical and Biophysical Research Communications* **70**, 381-388 (1976).
3. J. Saranak, K. W. Foster, Rhodopsin guides fungal phototaxis. *Nature* **387**, 465-466 (1997).
4. G. M. Avelar, R. I. Schumacher, P. A. Zaini, G. Leonard, T. A. Richards, S. L. Gomes, A rhodopsin-guanylyl cyclase gene fusion functions in visual perception in a fungus. *Curr Biol* **24**, 1234-1240 (2014).
5. K. H. Biswas, A. R. Shenoy, A. Dutta, S. S. Visweswariah, The evolution of guanylyl cyclases as multidomain proteins: conserved features of kinase-cyclase domain fusions. *J Mol Evol* **68**, 587-602 (2009).
6. T. C. Rich, T. E. Tse, J. G. Rohan, J. Schaack, J. W. Karpen, In vivo assessment of local phosphodiesterase activity using tailored cyclic nucleotide-gated channels as cAMP sensors. *J Gen Physiol* **118**, 63-78 (2001).
7. M. Stierl, P. Stumpf, D. Udvari, R. Gueta, R. Hagedorn, A. Losi, W. Gartner, L. Petereit, M. Efetova, M. Schwarzel, T. G. Oertner, G. Nagel, P. Hegemann, Light modulation of cellular cAMP by a small bacterial photoactivated adenylyl cyclase, bPAC, of the soil bacterium *Beggiatoa*. *J Biol Chem* **286**, 1181-1188 (2011).
8. W. Altenhofen, J. Ludwig, E. Eismann, W. Kraus, W. Bonigk, U. B. Kaupp, Control of ligand specificity in cyclic nucleotide-gated channels from rod photoreceptors and olfactory epithelium. *Proc Natl Acad Sci U S A* **88**, 9868-9872 (1991).

9. J. Y. Lin, M. Z. Lin, P. Steinbach, R. Y. Tsien, Characterization of Engineered Channel rhodopsin Variants with Improved Properties and Kinetics. *Biophysical Journal* **96**, 1803-1814 (2009).
10. K. A. Lucas, G. M. Pitari, S. Kazerounian, I. Ruiz-Stewart, J. Park, S. Schulz, K. P. Chepenik, S. A. Waldman, Guanylyl cyclases and signaling by cyclic GMP. *Pharmacol Rev* **52**, 375-414 (2000).
11. M. H. Ryu, O. V. Moskvina, J. Siltberg-Liberles, M. Gomelsky, Natural and engineered photoactivated nucleotidyl cyclases for optogenetic applications. *J Biol Chem* **285**, 41501-41508 (2010).
12. S. Raffelberg, L. Wang, S. Gao, A. Losi, W. Gartner, G. Nagel, A LOV-domain-mediated blue-light-activated adenylate (adenylyl) cyclase from the cyanobacterium *Microcoleus chthonoplastes* PCC 7420. *Biochem J* **455**, 359-365 (2013).
13. A. Berndt, O. Yizhar, L. A. Gunaydin, P. Hegemann, K. Deisseroth, Bi-stable neural state switches. *Nature Neuroscience* **12**, 229-234 (2009).
14. C. Bamann, R. Gueta, S. Kleinlogel, G. Nagel, E. Bamberg, Structural Guidance of the Photocycle of Channelrhodopsin-2 by an Interhelical Hydrogen Bond. *Biochemistry* **49**, 267-278 (2010).
15. A. Vogt, J. Wietek, P. Hegemann, Gloeobacter rhodopsin, limitation of proton pumping at high electrochemical load. *Biophys J* **105**, 2055-2063 (2013).
16. S. J. Guzman, A. Schlogl, C. Schmidt-Hieber, Stimfit: quantifying electrophysiological data with Python. *Front Neuroinform* **8**, 16 (2014).
17. C. Bamann, T. Kirsch, G. Nagel, E. Bamberg, Spectral characteristics of the photocycle of channelrhodopsin-2 and its implication for channel function. *Journal of Molecular Biology* **375**, 686-694 (2008).
18. L. Stoppini, P. A. Buchs, D. Muller, A simple method for organotypic cultures of nervous tissue. *J Neurosci Methods*. **37**, 173-182 (1991).
19. J. Rathenberg, T. Nevian, V. Witzemann, High-efficiency transfection of individual neurons using modified electrophysiology techniques. *J Neurosci Methods* **126**, 91-98 (2003).
20. B. A. Suter, T. O'Connor, V. Iyer, L. T. Petreanu, B. M. Hooks, T. Kiritani, K. Svoboda, G. M. Shepherd, Ephus: multipurpose data acquisition software for neuroscience experiments. *Front Neural Circuits*. **4**, 100 (2010).
21. J. D. Thompson, D. G. Higgins, T. J. Gibson, CLUSTAL W: improving the sensitivity of progressive multiple sequence alignment through sequence weighting, position-specific gap penalties and weight matrix choice. *Nucleic Acids Res* **22**, 4673-4680 (1994).
22. C. Cole, J. D. Barber, G. J. Barton, The Jpred 3 secondary structure prediction server. *Nucleic Acids Research* **36**, W197-W201 (2008).
23. M. Biasini, S. Bienert, A. Waterhouse, K. Arnold, G. Studer, T. Schmidt, F. Kiefer, T. G. Cassarino, M. Bertoni, L. Bordoli, T. Schwede, SWISS-MODEL: modelling protein

tertiary and quaternary structure using evolutionary information. *Nucleic Acids Research* **42**, W252-W258 (2014).

Acknowledgments: We thank Wolfgang Bönigk, Lena Geist, Rolf Hagedorn, Jeanine Klotz, Nicolas Liem, Iris Ohmert, Maila Reh, Christina Schnick, and Charlotte Wittig for excellent technical support. We are grateful to Dagmar Wachten for stimulating discussion and critical reading of the manuscript. **Funding:** This work was supported by the German Research Foundation, DFG (Cluster of excellence UniCat and SFB 1078 project B1 and B2 to PH, SPP1665 to PH and TGO) and by the IWT (Optobrain to PH). **Author contributions:** U.S. carried out all experiments in Oocytes including quantification of cGMP/cAMP. K.S. purified and carried out experiments with recombinant protein. C.G. carried out experiments in neurons. R.F. analyzed sequences. P.H. and T.O. designed experiments. U.S., K.S., C.G., T.O. and P.H. analyzed experiments and wrote the paper. **Competing interests:** none **Data and materials availability:** all data and material is freely available without MTA and plasmids will be available at AddGene.

Figures and Tables

Wavelength (nm)	Kinetic constants
380	$\tau_{\text{Rise}} = 8 \text{ ms} \pm 0.6 \text{ ms}$ $\tau_{\text{Decay}} = 93 \text{ ms} \pm 1 \text{ ms}$
505	$\tau_{\text{Rise 1}} = 0.38 \text{ ms} \pm 0.15 \text{ ms}$ $\tau_{\text{Rise 2}} = 9.2 \text{ ms} \pm 2.1 \text{ ms}$ $\tau_{\text{Decay 1}} = 104 \text{ ms} \pm 1 \text{ ms}$

	$\tau_{\text{Decay 2}} = 20 \text{ s} \pm 9.8 \text{ s}$
550	$\tau_{\text{Rise 1}} = 0.32 \text{ ms} \pm 0.19 \text{ ms}$ $\tau_{\text{Rise 2}} = 7.8 \text{ ms} \pm 0.59 \text{ ms}$ $\tau_{\text{Decay 1}} = 120 \text{ ms} \pm 2 \text{ ms}$ $\tau_{\text{Decay 2}} = 1.9 \text{ s} \pm 0.6 \text{ s}$

Table 1: Kinetic constants for the rise and decay of Rh-photocycle intermediates.

Fig. 1: Model of RhGC and activity in *Xenopus* oocytes. (A) Model of dimeric RhGC with 7 conserved TM helices (red) and two additional membrane spanning S-helices (beige). (B) Oocytes injected with 5 ng cGMP-sensitive CNG-A2 RNA and 2.5 ng RhGC (black traces) or truncated (tr) RhGC RNA (red trace) were irradiated for 2 seconds with 560 nm ($0.002 - 0.28 \text{ mW mm}^{-2}$ half band width 60 nm) show light intensity dependent inward currents at -40 mV. Current slopes were determined between 20-80 % of signal rise. (C) Normalized slopes ($n = 6$) plotted against light intensity were fit monoexponentially and EC_{50} was determined at 0.028 mW mm^{-2} (correlation $R^2 = 0.992$). (D) Stimulation of oocytes, injected with 5 ng RhGC-RNA and cGMP sensitive CNG-RNA, with 530 nm flashes of 0.006 mW mm^{-2} intensity and 0.1, 0.4, 0.7, 1.0, 1.3 and 1.6 second durations (-20 mV). (E) Enlargement of the grey region in panel (D) shows the initial current rise at different durations. (F) Stimulation for 30 seconds with 530 nm light at different intensities (-20 mV). (G) Lack of photocurrents in an oocyte coexpressing the cAMP-sensitive CNG-A2 (C460W/ E583M) variant and RhGC. When CNG-A2 (C460W/E583M) was instead coexpressed with bPAC, large photocurrents were induced (blue trace). Representative traces from $n \geq 5$ measurements are shown in (B-G). ELISA based detection of cGMP (H) and cAMP (I) in single oocytes 5 days after RNA injection. Oocytes were kept in the dark or illuminated for 5 min with 530 nm (0.010 mW mm^{-2}) or

450 nm (0.015 mW mm^{-2}). The amount of cGMP in the different groups was significantly different ($p < 0.0001$, Kruskal-Wallis) as was the amount of cAMP ($p = 0.001$, Kruskal-Wallis). Error bars, mean \pm sem, n : number of experiments with at least 3 oocytes each. $*P < 0.05$, $**P < 0.01$, $***P < 0.001$, $****P < 0.0001$, Mann-Whitney.

Fig. 2: Activity of RhGC stably expressed in CHO K1 cells. Fluorescence recordings in a 96-well microplate of CHO K1 cells stably coexpressing RhGC-mCherry and the cGMP sensitive CNG channel. (A) RhGC was stimulated for 50 s (black-dashed bar) by different numbers of flashes (30-2500, 485 nm, 1.3 W mm^{-2}) and Ca^{2+} - signals were monitored with Fluo-4. CHO cells solely expressing the cGMP sensor were used as a control (red) (mean of $n=3$ wells). (B) Repetitive stimulation (black arrows, 15 s, $1.3 \mu\text{W mm}^{-2}$) and recovery of the RhGC activity was monitored by Fura-2 in cells coexpressing the cGMP sensitive channel (curves are derived from 3 individual wells), rfu: relative fluorescence units.

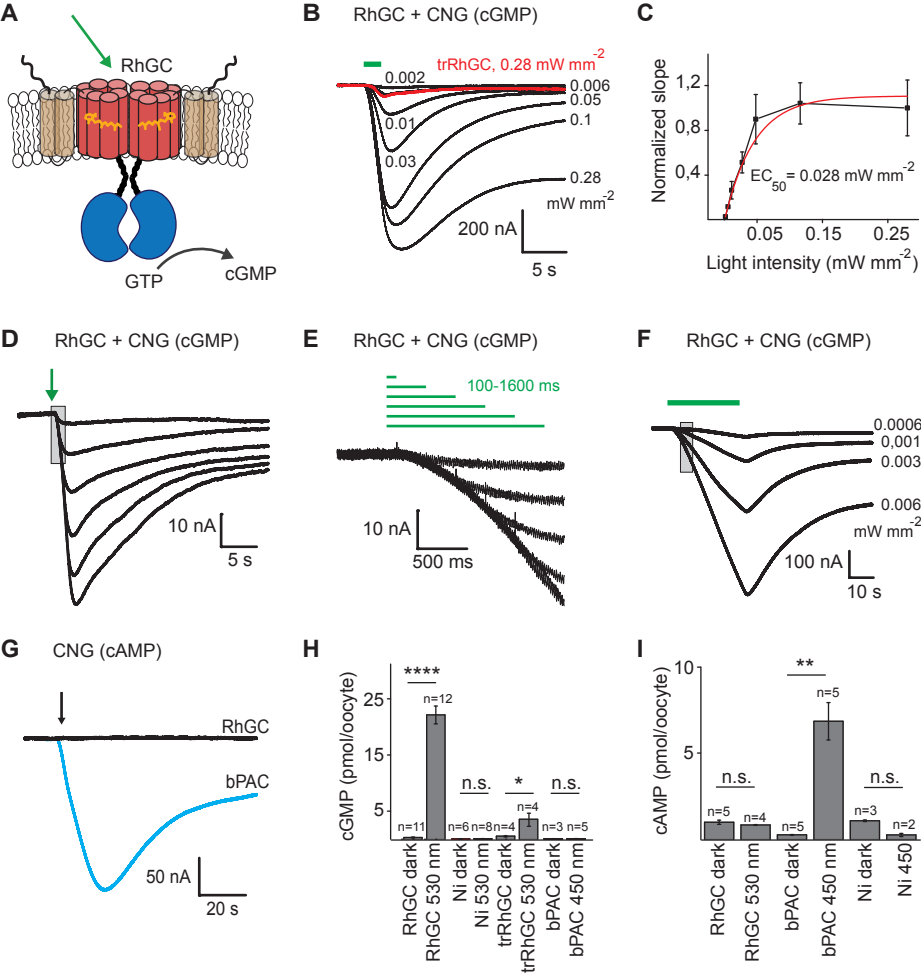
Fig. 3: Photochemical characterization and cGMP production. (A) Absorption spectrum of the recombinant rhodopsin fragment Rh in detergent at pH 8 before (black) and after (magenta) 1 minute illumination with 505 nm light (0.07 mW mm^{-2}) (B) Kinetics of 10 ns 525 nm laser flash-induced P380 formation and decay as well as depletion and recovery of D525 monitored at 505 and 550 nm (see also grey bars in A). (C) Reconstruction of time-resolved absorbance changes (colored) of Rh between 350 nm and 650 nm at pH 8 from 10^{-7} to 1 s after excitation with a 10 ns 525 nm laser flash. The analysis is based on the most significant components as obtained by singular value decomposition. (D) Aliquots were taken from a reaction mixture after 10 s, 30 s, 60 s, 120 s, 240 s, and 18 hours containing 10 μg green light exposed (\bullet) or dark adapted (\blacktriangle) RhGC-expressing

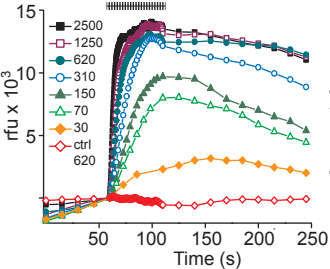
membrane and 1 mM GTP and were analyzed by HPLC. Integration of peak areas yielded initial reaction velocities. $**P < 0.01$, $***P < 0.001$.

Fig. 4: Light induced cGMP signaling in neurons expressing RhGC. (A) Fluorescence image of CA1 pyramidal neurons in hippocampal slice culture 10 days after electroporation with RhGC and mKate2. (B) Green light (530 nm, 19.2 mW mm^{-2} , 10 s) evoked currents that were less than -20 pA at -65 mV in cells expressing only RhGC (black trace, fast deflections are spontaneous synaptic events which were not blocked in this example). When the cGMP activated CNG-A2 channel was co-expressed, large inward currents were induced by light in neurons (red trace). (C) Photocurrent amplitude depends on the wavelength of sub-maximal light pulses (2 s, 1 mW mm^{-2}). (D) Summary of the activation spectra determined from $n = 6$ neurons. Boxes are median with 25 – 75 percentile, whiskers show minimum and maximum values. (E) Photocurrents evoked by brief light pulses (green ticks, 530 nm, 100 ms, 1 mW mm^{-2}) were fully reversible and reproducible at a frequency of 0.2 Hz.

Fig. 5: RhGC enables light dose-dependent control of cGMP in neurons. (A) CA1 neurons 7 days after electroporation with RhGC, the cGMP sensitive channel CNG-A2 and mKate2 (two photon microscopy, maximum intensity projection). (B, C) CA1 pyramidal neurons expressing RhGC and CNG-A2 showed normal spiking behavior in response to current steps (-400 to 400 pA). (D) Amplitude and slope of light-induced photocurrents increased with increasing light intensity (530 nm, 2s). Inset shows dose-response relationship for this example, curve generated with a logistic equation. (E) Normalized slope vs. light intensity ($n = 7$ neurons) was fit with a logistic equation. Hill slope = 0.994 (95%

confidence 0.758 to 1.23); $EC_{50} = 1.57 \text{ mW mm}^{-2}$ (95% confidence 0.88 to 1.52); $R^2 = 0.91$. (F) Light pulses of increasing length (530 nm, 19.2 mW mm^{-2}) elicited photocurrents of uniform slope and increasing amplitude. Saturation and inactivation of the responses became apparent during long light pulses. Inset shows close-up of the 100 ms to 1 s traces to illustrate how time to onset of response was measured. Traces in B, D and Fig. 4C are from the same cell. Traces in C and Fig. 4E are from the same cell.



A**B**